The influence of *Phaeocystis globosa* on microscale spatial patterns of chlorophyll *a* and bulk-phase seawater viscosity

**L. Seuront · C. Lacheze · M. J. Doubell ·
J. R. Seymour · V. Van Dongen-Vogels ·
K. Newton · A. C. Alderkamp · J. G. Mitchell**

Abstract A two-dimensional microscale (5 cm resolution) sampler was used over the course of a phytoplankton spring bloom dominated by *Phaeocystis globosa* to investigate the structural properties of chlorophyll *a* and seawater excess viscosity distributions. The microscale distribution patterns of chlorophyll *a* and excess viscosity were never uniform nor random. Instead they exhibited different types and levels of aggregated spatial patterns that were related to the dynamics of the bloom. The chlorophyll *a* and seawater viscosity correlation patterns were also controlled by the dynamics of the bloom with positive and negative correlations before and after the formation of foam in the turbulent surf zone. The ecological relevance and implications of the observed patchiness and biologically induced increase in seawater viscosity are discussed and the combination of the enlarged colonial form and mucus secretion is suggested as a competitive advantage of *P. globosa* in highly turbulent environments where this species flourishes.

L. Seuront (✉) · C. Lacheze
CNRS FRE 2816 ELICO, Station Marine de Wimereux, University of Sciences and Technologies of Lille-Lille 1, 28 avenue Foch, 62930 Wimereux, France
e-mail: Laurent.Seuront@univ-lille1.fr

L. Seuront · M. J. Doubell · K. Newton · J. G. Mitchell
School of Biological Sciences, Flinders University, GPO Box 2100, Adelaide, SA 5001, Australia

J. R. Seymour
Department of Civil and Environmental Engineering, Massachusetts Institute of Technology, 77 Massachussets Avenue, Cambridge, MA 02139-4307, USA

V. Van Dongen-Vogels
Marine Biology Laboratory, Catholic University of Louvain, Batiment Kellner, 3 Place Croix du Sud, Louvain-La-Neuve 1348, Belgium

A. C. Alderkamp
Department of Marine Biology, University of Groningen, PO Box 14, Haren 9750AA, The Netherlands

Introduction

Plankton patchiness is widely acknowledged as a ubiquitous and key feature of marine ecosystems (Martin 2003). Many organisms have been shown to exploit patches of food (e.g., Tiselius 1992), and patch formation may be important in the foraging success of many marine invertebrates (Seuront et al. 2001) and vertebrates (Cartamil and Lowe 2004), as well as for the sexual encounters among individuals of relatively rare species (Buskey 1998). While the quantification of the spatial and temporal structure of phytoplankton distributions has for the most part focussed on empirical observations at scales greater

than 10 m to several kilometres (Martin 2003), there is a growing evidence for the existence of both vertical and horizontal phytoplankton patchiness at scales smaller than one metre (e.g., Dekshenieks et al. 2001). Because the analysis of large-scale patterns must integrate processes occurring at much smaller scales (Levin 1992), investigating the physical and biological dynamics controlling microscale plankton patchiness may be an absolute prerequisite to improve our understanding of the scales, intensities, durations and ecological relevance of these patterns.

The cosmopolitan genus *Phaeocystis* is a key organism in driving global geochemical cycles, climate regulation and fisheries yield (Schoemann et al. 2005), and has recently been suggested as a potential source of microscale phytoplankton patchiness (Seuront 2005). Of particular importance is the formation of large, gel-like colonies (from several mm to several cm; Verity and Medlin 2003) which form thick brown jelly layers (Al-Hasan et al. 1990) that modify the rheological properties of seawater, produce foam that resembles whipped egg white (Dreyfuss 1962), and clog plankton and fish nets (Peperzak 2002). Large quantities of foam are generated in the turbulent surf zone of beaches along the North Sea and the Eastern English Channel (Lancelot et al. 1987; Seuront et al. 2006). Quantitative descriptions of the bulk-phase properties of seawater during phytoplankton blooms have estimated the changes in the viscous properties of seawater that are induced by phytoplankton mucus secretion (Jenkinson 1986, 1993; Jenkinson and Biddanda 1995; Seuront et al. 2006), and found a positive correlation between seawater viscosity and chlorophyll *a* concentration during *Phaeocystis* sp. blooms in the German Bight and the North Sea (Jenkinson 1993; Jenkinson and Biddanda 1995). More recent work (Seuront et al. 2006) showed a significant increase in seawater viscosity with the development of a *Phaeocystis globosa* bloom in the Eastern English Channel, and a positive correlation between chlorophyll concentration and seawater viscosity before foam formation as well as a negative correlation after foam formation. These results suggest that seawater viscosity is influenced by extracellular materials associated with colony formation and colony maintenance rather than by cell composition and standing stock.

In this context, the aim of this study is to use a microscale (5 cm resolution) two-dimensional sampler to investigate: (i) the heterogeneity of the microscale distributions of phytoplankton biomass and bulk-phase seawater viscosity, (ii) the potential changes in these distributions over the course of a *P. globosa* spring bloom and (iii) the nature of the correlation between seawater viscosity and phytoplankton before, during and after the formation of foam in the turbulent surf zone.

Materials and methods

Study site

Samples were taken from the end of a coastal pier situated in the intertidal waters of the French coast of the Eastern English Channel, approximately 20 m from the shoreline (50°45′896″ N, 1°36′364″ E), near Boulogne-sur-Mer (France). The Eastern English Channel is characterised by 3 to 9 m tides. These tides are characterised by a residual translation parallel to the coast, with nearshore coastal waters drifting from the English Channel into the North Sea. Coastal waters are influenced by freshwater run-off from the Seine estuary to the Straits of Dover. This coastal flow (Brylinski et al. 1991) is separated from offshore waters by a tidally maintained frontal area. The coastal flow water mass is characterised by its low salinity, high turbidity, high phytoplankton richness and high productivity compared to the oceanic offshore waters (Seuront 2005). This sampling site was chosen because the physical and hydrological properties are representative of the inshore water masses of the Eastern English Channel (Seuront 2005). Sampling was conducted at high tide, before, during and after the *Phaeocystis globosa* bloom in the Eastern English Channel on 26 September 2003, 5 March 2004, 18 March 2004, 1 April 2004, 20 April 2004, 10 May 2004, 25 May 2004 and 20 June 2004.

Microscale sampling device

A purpose-designed two-dimensional (2D) sampling device was developed to investigate the microscale distributions of chlorophyll *a* and seawater viscosity.

The design of the device was based on sampling systems previously employed to measure the microscale spatial distributions of bacteria and phytoplankton (Seymour et al. 2000; Waters et al. 2003) and consisted of a 10 × 10 array of 50 ml syringes, separated by 5 cm and with a 3 mm wide opening. The pneumatically operated device was attached to a series of electric pumps allowing for the simultaneous collection of 100 samples across an area of 0.2 m^2. On retrieval, a polyvinyl chloride (PVC) rack holding 60 ml vials was inserted below the syringe array on stainless-steel rails, and the samples were transferred into the vials, which were immediately brought back to the laboratory in a cooler, stored in the dark in a room at the in situ temperature; all subsequent analysis were conducted within 2 h to avoid potential biases related to exudation during temperature changes and in high light. Samples were taken from a depth of 1 m, and the temperature and salinity of each water sample was measured using a Hydrolab probe at each of the sampling dates. The presence and the size of *P. globosa* colonies were investigated from bulk seawater samples taken simultaneously to the microscale samples.

Chlorophyll *a* analysis

Chlorophyll concentrations were estimated from 40 ml subsamples following Suzuki and Ishimaru (1990). Samples were filtered on Whatman GF/F glass-fibre filters (pore size 0.45 μm). Chlorophyllous pigments were extracted by direct immersion of the filters in 5 ml of N,N-dimethylformamide, and actual extractions were made in the dark at −20°C. Concentrations of chlorophyll *a* in the extracts were determined following Strickland and Parsons (1972) using a Turner 450 fluorometer previously calibrated with chlorophyll *a* extracted from *Anacystis nidulans* (Sigma Chemicals, St Louis).

Bulk-phase seawater viscosity measurements

Viscosity measurements were conducted using a portable ViscoLab400 viscometer (Cambridge Applied Systems Inc., Boston) from 10 ml subsamples following Seuront et al. (2006). Viscosity was measured in triplicate from 3 ml water subsamples poured into a small chamber, where a low-mass stainless-steel piston is magnetically forced back and

forth, with a 230 μm piston-cylinder gap size. The force driving the piston is constant, and the time required for the piston to move back and forth into the measurement chamber is proportional to the viscosity of the fluid. The more viscous the fluid the longer it takes the piston to move through the chamber, and vice versa. As viscosity is influenced by temperature and salinity (Miyake and Koizumi 1948), the measured viscosity η_m (cP) can be thought of as the sum of a physically controlled viscosity component $\eta_{T,S}$ (cP) and a biologically controlled viscosity component η_{Bio} (cP) (Jenkinson 1986):

$$\eta_m = \eta_{T,S} + \eta_{\text{Bio}} \tag{1}$$

The physically controlled component $\eta_{T,S}$ was estimated from viscosity measurements conducted on subsamples after passing through 0.20 μm pore size filters. The biologically induced excess viscosity η_{Bio} (cP) was subsequently defined from each water sample as:

$$\eta_{\text{Bio}} = \eta_m - \eta_{T,S} \tag{2}$$

The relative excess viscosity η (%) is finally given as (Seuront et al. 2006):

$$\eta = (\eta_m - \eta_{T,S})/\eta_{T,S} \tag{3}$$

Before each viscosity measurement, temperature and salinity of the water sample were simultaneously measured using a Hydrolab probe, and did not exhibit any significant difference with the theoretical viscosity estimated from temperature and salinity (Wilcoxon–Mann–Whitney *U*-test, $P > 0.05$). This ensures the relevance of our $\eta_{T,S}$ estimates. Between each viscosity measurement, the viscometer chamber was carefully rinsed first with deionised water and then with bulk-phase seawater filtered through 0.2 μm pore size filters to avoid any potential dilution of the next sample.

Potential biases and limitations

Due to the difficulty in handling *Phaeocystis* sp. colonies without disrupting them, our viscosity measurements could have been biased through the disruption of colonies: (i) during the sampling process and/or (ii) the viscosity measurement in the

chamber of the viscometer. This would result in creating additional mucus particles and releasing additional macromolecules into solution, and thus a biased increase in seawater viscosity. These two potential issues have been carefully addressed to ensure the relevance of our viscosity measurements.

Any *P. globosa* colony larger than the opening of the syringes (i.e. 3 mm) would be destroyed during the sampling. This is unlikely to have occurred during our sampling for two reasons. First, the size of *P. globosa* colonies in bulk samples taken simultaneously to our 2D sampling, observed by inverted microscopy and measured using an ocular micrometer, ranged in size from 0.1 to 1.3 mm at concentrations ranging from 500 to 5,000 per litre (Table 1). Control measurements were carried out at each of our sampling dates, during which we compared the viscosity measured from water samples taken by the syringes of the 2D sampler and from bulk seawater samples. As no significant differences were found between the two estimates (Wilcoxon–Mann–Whitney *U*-test, $P > 0.05$, $N = 100$), the syringe sampler has not been considered as a potential source of bias in subsequent viscosity measurements.

Fragile colonies, and more specifically the colonies larger than 230 μm (as the piston-cylinder gap is only 230 μm; see above) would still be destroyed in the measurement chamber, and would result in a biased increase in seawater viscosity. Therefore all visible *P. globosa* colonies were systematically removed from the 3 ml samples with a Pasteur pipette under a dissecting microscope (magnification × 100), under temperature controlled conditions before viscosity measurements were conducted. Considering the relatively large colonies at relatively low concentrations (500 to 5000 per litre; Table 1) we can assume that most though maybe not all colonies were removed. It could also be argued here that this could have been achieved through a careful screening of the water samples through a 200 μm mesh before doing the measurements. However, a 200 μm screening would still not remove the colonies smaller than 200 μm that are still likely to be destroyed by the high shear occurring in the measurement chamber and to create additional mucus particles and release additional macromolecules into solution. The two methods are then both potentially biased, but in similar ways, as preliminary testing conducted

Table 1 Mean abundance (colonies l^{-1}) and size (μm) of *P. globosa* colonies observed at each sampling date

Date	*Phaeocystis globosa* colonies			
	Size (μm)	N_1	Abundance (col l^{-1})	N_2
26/09/03	–	–	0	–
05/03/04	–	–	0	–
10/03/04	–	–	0	–
01/04/04	180 (100–220)	100	1400(1200–1600)	5
20/04/04	270(230–660)	100	1200(990–1350)	4
10/05/04	500 (300–1300)	100	5000(4820–5250)	4
25/05/04	390 (300–645)	100	500(290–560)	4
20/06/04	–	–	0	–

The values given in parenthesis are the minimum and maximal values. N_1 is the number of colonies considered for size measurements and N_2 is the number of bulk samples used to estimate colony abundance

during the 2002 and 2003 spring blooms did not exhibit any significant difference (Fig. 1). Finally, we have already shown a distinct increase in excess seawater viscosity following the mechanical disruption of *P. globosa* colonies (Seuront et al. 2006). This would not have been possible if just the act of making a measurement increased viscosity.

Data analyses

Quantifying microscale spatial variability. A simple quantification of the degree of microscale variability observed for a given 2D microscale distribution was expressed as the ratio between maximum and minimum values of the distributions, considered as an estimate of the maximum variability (Seuront and Spilmont 2002), and the coefficient of variation CV (CV = SD/$\bar{x}$, where $\bar{x}$ and SD are the mean and the standard deviation, respectively) estimated for that range.

Identifying spatial structure

Spatial autocorrelation analysis was used to quantify patterns in two-dimensional microscale distribution of chlorophyll *a* concentrations (μgChl-a l^{-1}) and relative seawater excess viscosity η (%). The objective is to link these parameters to a common patch size to quantify their spatial linkage.
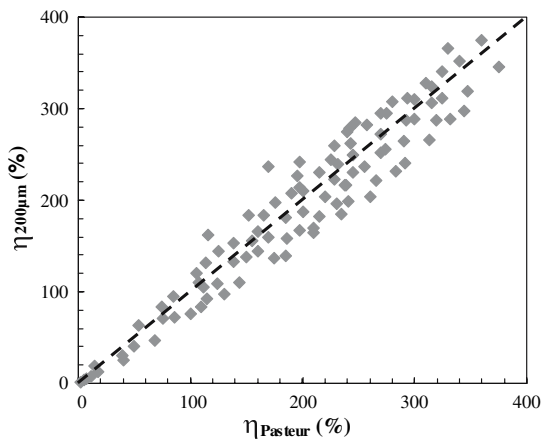
Fig. 1 Comparisons of the excess viscosity measurements η (%) obtained from bulk phase seawater samples after removing all the visible colonies from the water samples with a Pasteur pipette under a dissecting microscope (magnification × 100), $\eta_{Pasteur}$, and after carefully screening the water samples through a 200 μm mesh ($\eta_{200\mu m}$) before doing the measurements. A modified t-test (Zar 1996) did not exhibit a significant difference between our measurements and the theoretical expectation $\eta_{Pasteur} = \eta_{200\mu m}$ ($P > 0.05$, $N = 100$)

Generally speaking, positive spatial autocorrelation indicates that abundances in adjacent localities are similar (aggregation) while negative-autocorrelation signifies that adjacent localities alternate between high and low values, i.e. peaks and valleys, and hot spots and cold spots. The theory and use of spatial autocorrelation procedures to analyse spatial associations has been extensively discussed (Sokal and Oden 1978a, b), and the reader is referred to these papers for more-detailed descriptions.

Moran's I and Geary's c spatial autocorrelation statistics (Moran 1950; Geary 1954) are defined as:

$$I(d) = \frac{\frac{1}{W}\sum_{i=1}^{n}\sum_{j=1}^{n}w_{ij}(y_i - \bar{y})(y_j - \bar{y})}{\frac{1}{n}\sum_{i=1}^{n}(y_j - \bar{y})^2} \text{ for } i \neq j \qquad (4)$$

and

$$c(d) = \frac{\frac{1}{2W}\sum_{i=1}^{n}\sum_{j=1}^{n}w_{ij}(y_i - y_j)^2}{\frac{1}{(n-1)}\sum_{j=1}^{n}(y_j - \bar{y})^2} \text{ for } i \neq j \qquad (5)$$

where y_i and y_j are the values of the observed variable at sites i and j, $\bar{y}$ is their mean and W is defined as

$W = \sum_{i}^{n}\sum_{j}^{n}w_{ij}$ where $w_{ij} = d_{ij}^{-2}$ when sites i and j are at a distance d and $w_{ij} = 0$ otherwise. Only the pairs of site (i, j) within the stated distance class (d) are taken into account.

Moran's I Eq. 4 and Geary's c Eq. 5 are two related, but conceptually different, autocorrelation coefficients. Moran's I, which ranges from +1 to −1, is sensitive to extreme abundances in nearby localities while Geary's c, bounded between 0 and an unspecified value larger than 1, indicates whether nearby localities exhibit similar abundances. A positive autocorrelation (i.e. positive values of I) indicates dependence between samples that are spatially close. In contrast, a negative autocorrelation (i.e. negative values of I) indicates dependence between distant samples. The no-correlation values is thus $I = 0$. A Geary's c correlogram varies as the reverse of a Moran's I correlogram: strong autocorrelation produces high values of I and low values of c. Positive autocorrelation translates into values of c between 0 and 1 whereas negative autocorrelation produces values larger than 1. Hence, the reference no-correlation value is $c = 1$.

Under the hypothesis of a random spatial distribution, the expected values of the Moran's I and Geary's c are $I = -(n - 1)^{-1}$ and $c = 1$, respectively. When combined with the Fisher's dispersion index ($S^2/\bar{x}$ or variance-to-mean ratio), Moran's I and Geary's c were used to characterise and classify in an objective way the spatial pattern of a particular descriptor (see Table 2). In addition, patch sizes were determined from spatial correlograms, i.e. Moran's I plotted against the separation distance d. As a minimum number of 30 pairs are necessary to estimate autocorrelation statistics with confidence (Legendre and Legendre 1998), nine distance classes were used, with distances ranging from 5 to 45 cm. The significance of spatial correlograms was tested using the Bonferroni-corrected significance procedure (Legendre and Legendre 1998). For each 2D data set, the distance at which I changes sign was used as an estimate of the average patch radius (Sokal and Oden 1978a).

Statistical analyses

For each date, the chlorophyll a distribution and seawater viscosity data were significantly non-normally distributed (Kolmogorov–Smirnov test,

Table 2 Types of distribution patterns based on values of Moran's *I*, Geary's *c* and variance-to-mean ratio. S indicates that the value is significantly different from the expected value, while NS denotes no significant difference

Type	I	c	$S^2/\bar{x}$	Distribution
A	S	S	–	Transition from high to low abundance occurs within the sampling area, i.e. gradient in abundance
B	S–	S–	S–	Uniform
C	S	NS	–	Aggregative, based on a few extreme peaks in abundance
D	NS	S	–	Aggregative, based on several similar peaks in abundance
E	NS	NS	S+	Aggregative, due to high abundance in a single, isolated location
F	NS	NS	NS	Random

The + and − signs indicate whether the value is higher or lower than the expected value, respectively. Conclusions are based on discussions contained in Sokal and Oden (1978a), and Decho and Fleeger (1988)

$P < 0.01$), so nonparametric statistics were used throughout this work. Simple comparisons between two parameters were conducted using the Wilcoxon–Mann–Whitney (WMW) test. Correlation between variables was investigated using Kendall's coefficient of rank correlation, τ. Kendall's coefficient of correlation was used in preference to Spearman's coefficient of correlation ρ because Spearman's ρ gives greater weight to pairs of ranks that are further apart, while Kendall's τ weights each disagreement in rank equally (Sokal and Rohlf 1995).

Results

Environmental conditions

Salinity did not exhibit any characteristic pattern and fluctuated between 35.1 and 35.3 PSU (35.20 ± 0.02 PSU; $\bar{x} \pm$ SD). Temperature exhibited a clear seasonal cycle, ranging from 6.1°C on March 5 to 17.2°C on September 26.

Microscale spatial variability

The temporal patterns of chlorophyll *a* concentration and seawater excess viscosity are summarised in Table 3. Chlorophyll concentration and seawater excess viscosity were below 3.0 µg Chl-*a* l^{-1} on September 26 and March 5 (Table 3). Chlorophyll concentration then exhibited a sharp increase, corresponding to the initiation and the development of the spring bloom, to reach a maximum value of

57.4 ± 6.5 µg Chl-*a* l^{-1} ($\bar{x} \pm$ SD) on May 10, followed by a 3.5-fold decrease between May 10 and May 25 that coincided with the formation of foam in the turbulent surf zone. In contrast, seawater excess viscosity reached its peak (28 ± 25%; $\bar{x} \pm$ SD) on May 25 after the beginning of foam formation, and finally sharply decreased down to 5 ± 3% on June 20.

The values of the coefficient of variation (CV) and the ratios between maximum and minimum values (max./min.) demonstrate the high variability of microscale 2D distributions of chlorophyll *a* biomass and seawater excess viscosity (Table 3). The variability of chlorophyll and excess viscosity 2D distributions were minimum during the formation of foam in the turbulent surf zone. As further illustration of this variability, the 5 cm resolution, two-dimensional distributions of chlorophyll *a* concentration and seawater excess viscosity are shown for the pre-bloom condition (Fig. 2a), during the spring bloom, before (Fig. 2b) and after (Fig. 2c) the formation of foam in the turbulent surf zone, and after the bloom (Fig. 2d). Chlorophyll concentration and excess viscosity show alternating high- and low-density areas separated by sharp gradients and characterised by localised hot spots and cold spots (Fig. 2). The differential effect of foam formation on the two-dimensional distributions of chlorophyll *a* and excess viscosity is also clear from the transition observed between the pre- and post-foam distributions (Fig. 2b, c). Before the formation of foam, chlorophyll *a* and excess viscosity distributions are dominated by a high-density background and a few cold spots (Fig. 2b), while after the formation of foam, the chlorophyll *a* distributions were dominated by a
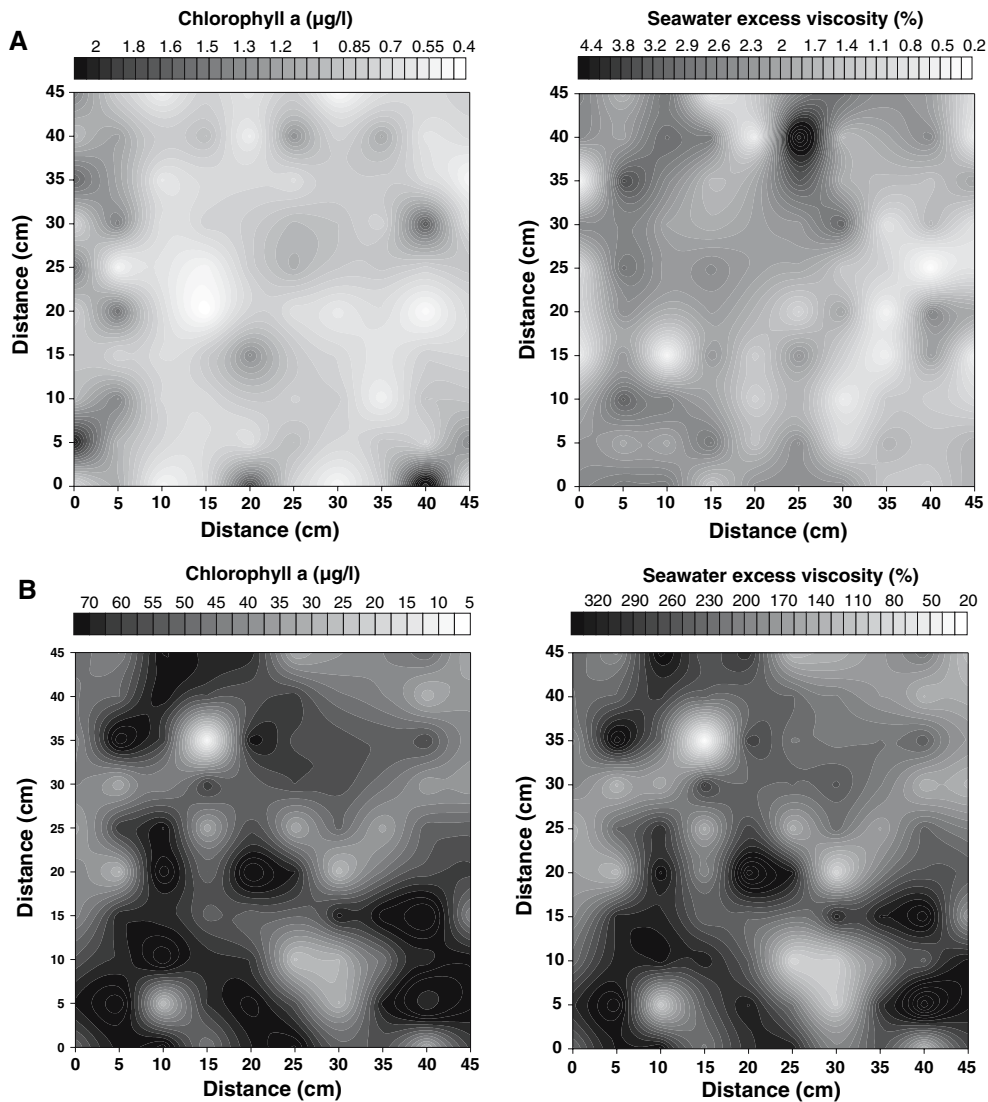
Fig. 2 Two-dimensional distributions of chlorophyll *a* concentrations (μg l^{-1}) and seawater excess viscosity (%) before the spring phytoplankton bloom (**A**) and during the spring bloom before foam formation in the turbulent surf zone (**B**).

Two-dimensional distributions of chlorophyll *a* concentrations (μg l^{-1}) and seawater excess viscosity (%) during the spring phytoplankton bloom after foam formation in the turbulent surf zone (**C**), and after the bloom (**D**)

low-density background and a few hot spots (Fig. 2c). Finally, the chlorophyll biomass and excess viscosity do not show any clear correlation pattern in pre- and post-bloom conditions (Fig. 2a, d). In contrast, they exhibit positive and negative correlation before and after the formation of foam, respectively (Fig. 2b, c).

Microscale spatial correlation

To identify any possible correlation between chlorophyll concentration and excess viscosity, excess viscosity was plotted against chlorophyll *a* concentration (Fig. 3). In pre-bloom conditions (September 26), no relationship is visible between chlorophyll concentration and excess viscosity. The development of the spring bloom is subsequently clearly visible, with simultaneous increases in chlorophyll *a* concentration and excess viscosity from March 5 to April 20. After the formation of foam, a progressive decoupling between chlorophyll concentration and excess viscosity occurred. It was initiated on May 10, when positive and negative correlations were observed
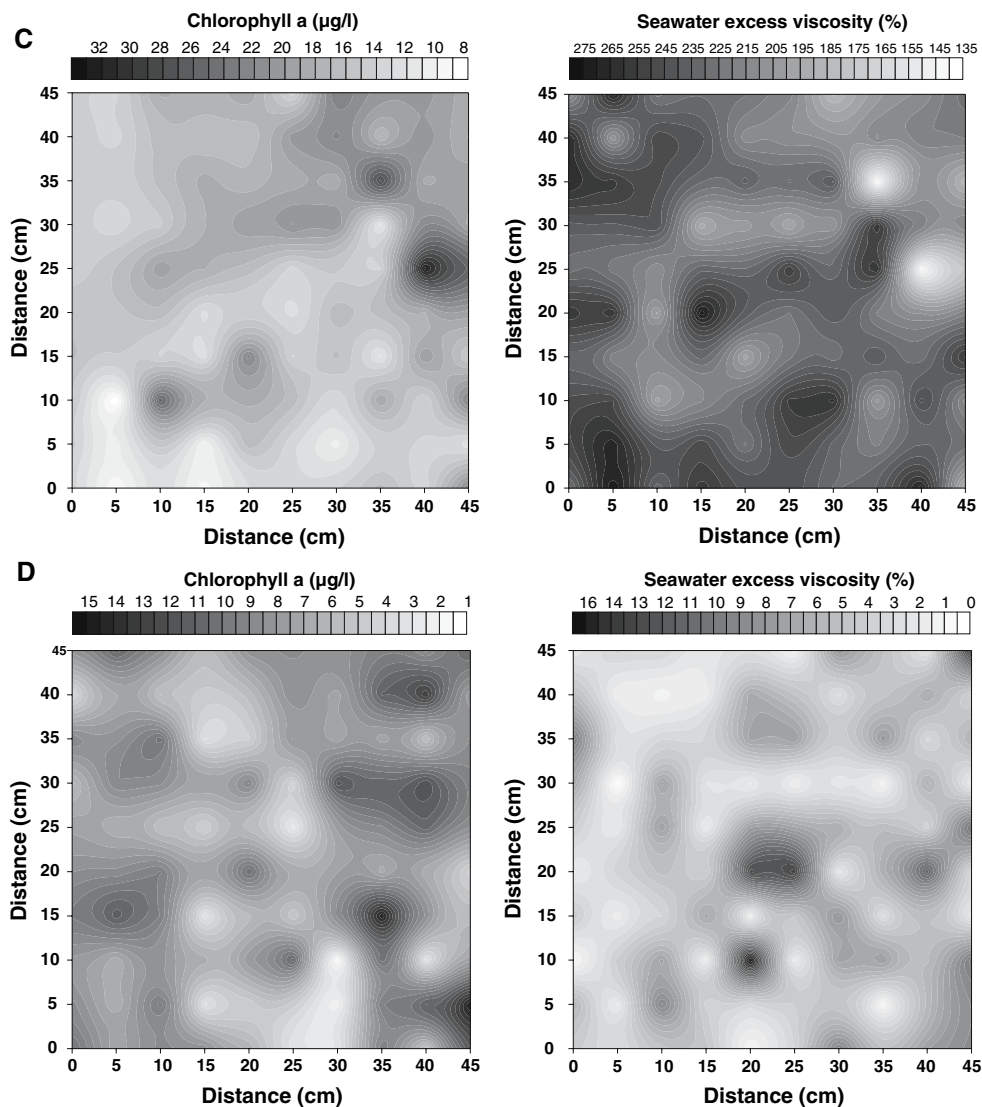
Fig. 2 continued

between chlorophyll concentration and excess viscosity for chlorophyll concentrations higher and lower than 55 µg Chl-a l^{-1}, respectively. On May 25, accompanying a sharp decrease in Chl-a concentration, excess viscosity was negatively related to chlorophyll concentration. Finally, in post-bloom conditions (June 20), chlorophyll concentration and excess viscosity appeared independently distributed. These observations are specified by the values of Kendall rank correlation coefficients (Fig. 4) estimated at each date between the two distributions. No significant correlation was observed in pre- and post-bloom conditions, while significant positive and

negative correlations were observed during the spring bloom before and after the formation of foam, respectively (Fig. 4).

Microscale spatial structure

The results of spatial autocorrelation analysis showed that none of the investigated patterns were uniform nor random (Table 4), indicating the existence of structural complexity in 2D microscale patterns of chlorophyll a concentration and seawater viscosity. Except on June 20, consistent spatial patterns were found for chlorophyll and excess
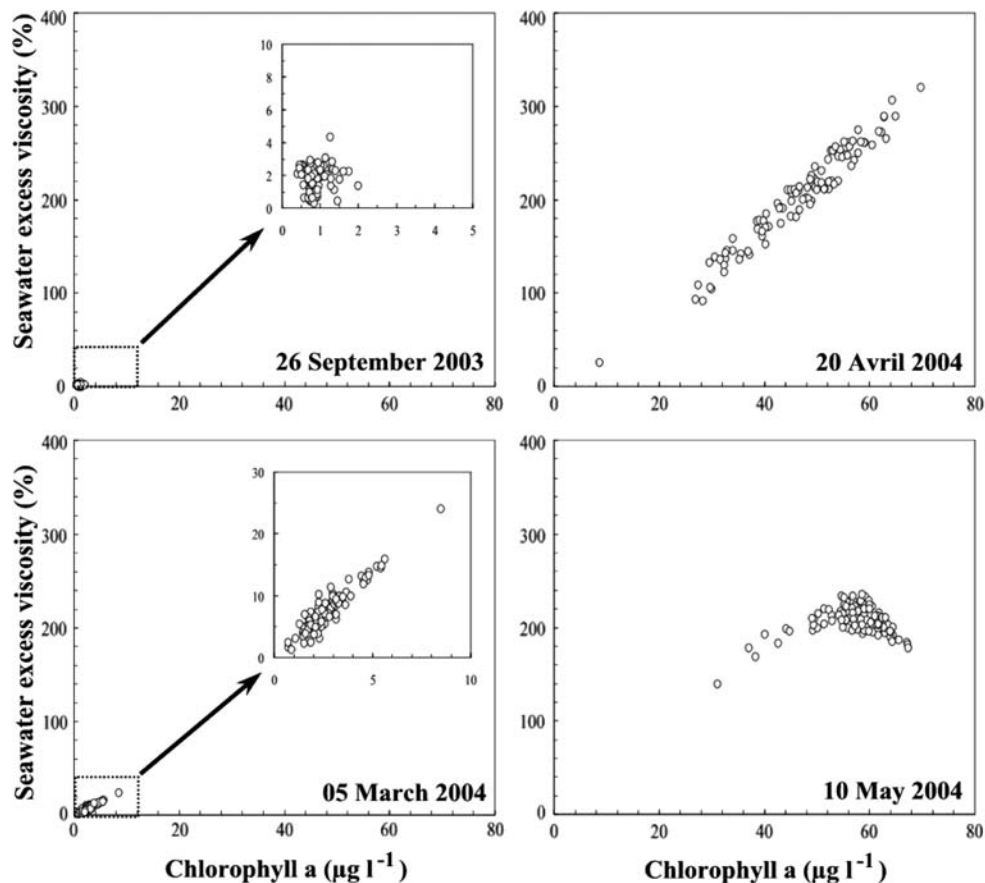
Fig. 3 Scatterplots of seawater excess viscosity η (%) as a function of chlorophyll *a* concentration ($\mu g\ l^{-1}$), showing the two different regimes observed over the course of our survey. The sampling conducted on 26 September has been used as a separate reference sample, characteristic of non-bloom conditions. Scatterplots of seawater excess viscosity η (%) as a function of chlorophyll *a* concentration ($\mu g\ l^{-1}$), showing the two different regimes observed over the course of our survey

viscosity. More specifically, pre- and post-bloom conditions were mainly characterised by three types of aggregative distributions (Table 4). In contrast, the spatial patterns observed during the bloom were either aggregative (i.e. dominated by the presence of a few extreme peaks) or characterised by a variety of transitions from high to low values, the latter being only observed during the formation of foam. Patch sizes were finally estimated from correlograms constructed for each parameter at each date to determine spatial autocorrelation as a function of increasing distance between samples. Because the distance intervals were based on the distance intervals between the centre points of samples, patch sizes were expressed in terms of the distance interval in which the autocorrelation value changed sign (positive to negative autocorrelation or vice versa). Patch sizes for chlorophyll concentration and excess viscosity were between 5 and 10 cm in pre- and post-bloom conditions (Table 4). Larger patch sizes were found for chlorophyll concentration and excess seawater viscosity in bloom conditions. During the formation of foam viscous patches were larger than chlorophyll patches (Table 4).

Discussion

Microscale spatial patterns and Phaeocystis globosa bloom dynamics

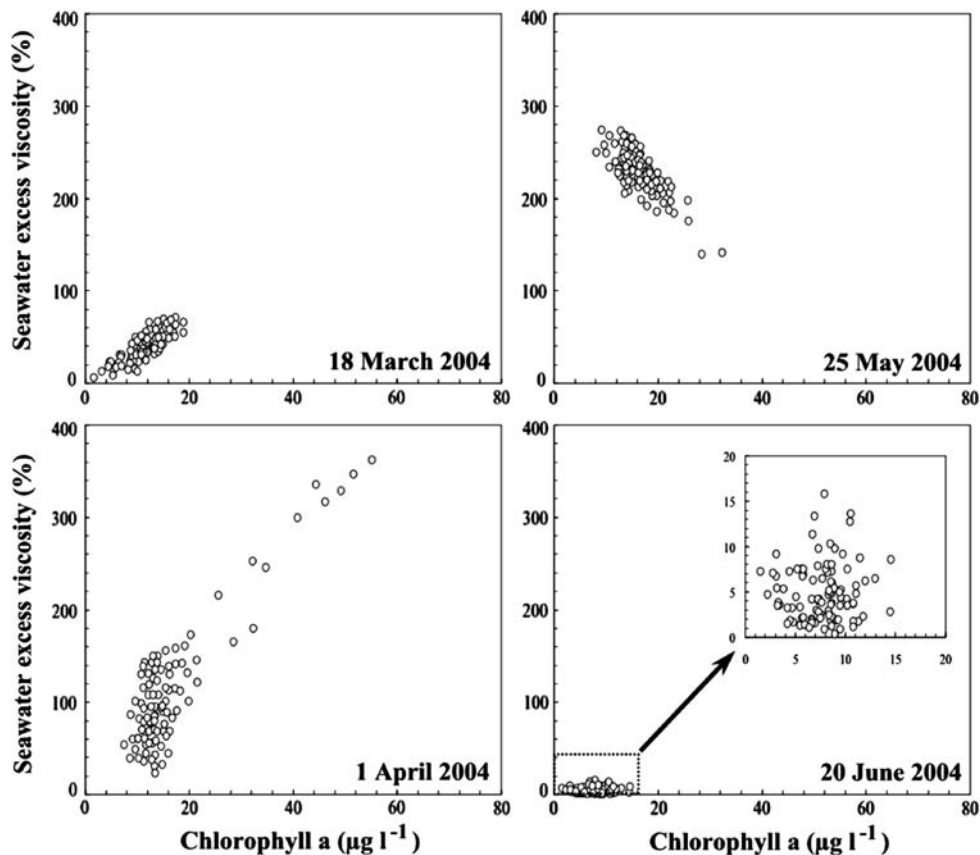*Chlorophyll, viscosity and foam formation.* The shift from significant positive correlations to significant

Fig. 3 continued

negative correlations before and after the foam formation is congruent with a recent mechanistic explanation (Seuront et al. 2006), suggesting that the disruption of the mucilaginous colonial matrix by turbulent mixing in the surf zone leads: (i) to the formation of foam and to the transformation of colonial cells into flagellated ones (Peperzak 2002), (ii) to a decrease in chlorophyll *a* concentration (Fig. 5) as a significant proportion of cells are entrained within the foam during the emulsion process (Seuront et al. 2006), and finally (iii) to the decoupling between the viscous (i.e. colonial polymeric materials) and nonviscous (flagellated cells) contribution of *P. globosa* to bulk-phase seawater properties in intertidal (Fig. 5a, b) and inshore (Fig. 5c, d) water masses, located respectively 20 m and 2 nautical miles from the shoreline. However, the relationship observed between chlorophyll concentration and excess viscosity on May 10 through our microscale sampling strategy (Fig. 3) indicates that the aforementioned

decoupling process could be more complex than initially thought. As the negative correlation occurs for the chlorophyll *a* concentrations higher than 55 µg l^{-1}, the high-density chlorophyll patches, likely to be the largest and/or the oldest ones, may be more fragile and thus the first ones to be destroyed by turbulent mixing. This hypothesis is consistent with the strong decrease in variability and the changes in the distribution patterns observed in both chlorophyll and excess viscosity spatial patterns between April 20 and May 10 (see Tables 3 and 4, Fig. 5a, b).

The mechanistic explanation proposed above for the dynamics of chlorophyll *a* concentration and seawater excess viscosity is also consistent with recent work conducted on the dynamics of transparent exopolymeric particles (TEP) produced by *Phaeocystis globosa* (Mari et al. 2005). Two phases for the dynamics of TEP were then identified: (i) a production phase during the growth phase of *P. globosa* where TEP and chlorophyll *a* concentration were
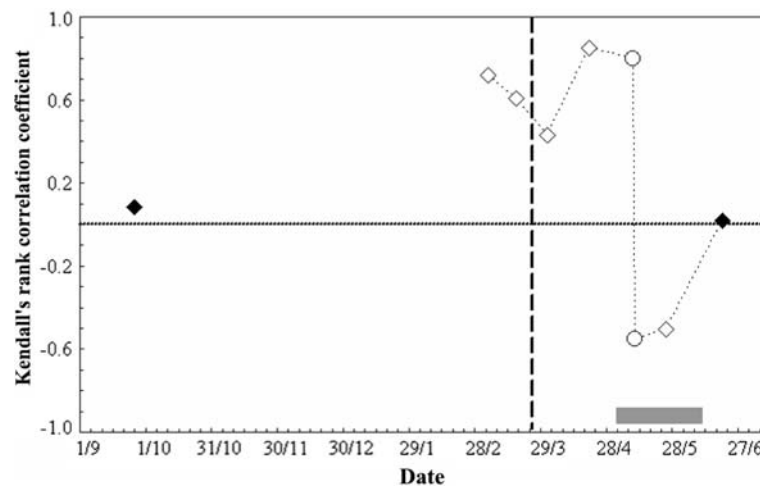
Fig. 4 The time course of the Kendall's correlation coefficient τ, estimated between the 100 simultaneous measurements of chlorophyll concentrations and seawater viscosity at each sampling date. The open and black diamonds represent significant (P < 0.05) and nonsignificant Kendall's τ, and the

open dots the two correlation patterns observed on May 10 (see Fig. 2). The grey bar indicates the period of foam formation (May 3 to June 10). The sampling conducted on 26 September has been used as a separate reference sample, characteristic of non-bloom conditions

positively correlated, and (ii) a release of large TEP from the mucilaginous matrix of *P. globosa* colonies subsequent to colony disruption (caused by nutrient depletion) where TEP and chlorophyll *a* concentration were negatively correlated. The causes of colony

disruption observed by Mari et al. (2005) and the area described in the present work might diverge. The similarity between the dynamics of chlorophyll *a* concentration-excess viscosity shown in the present work and chlorophyll *a* concentration-TEP concen-
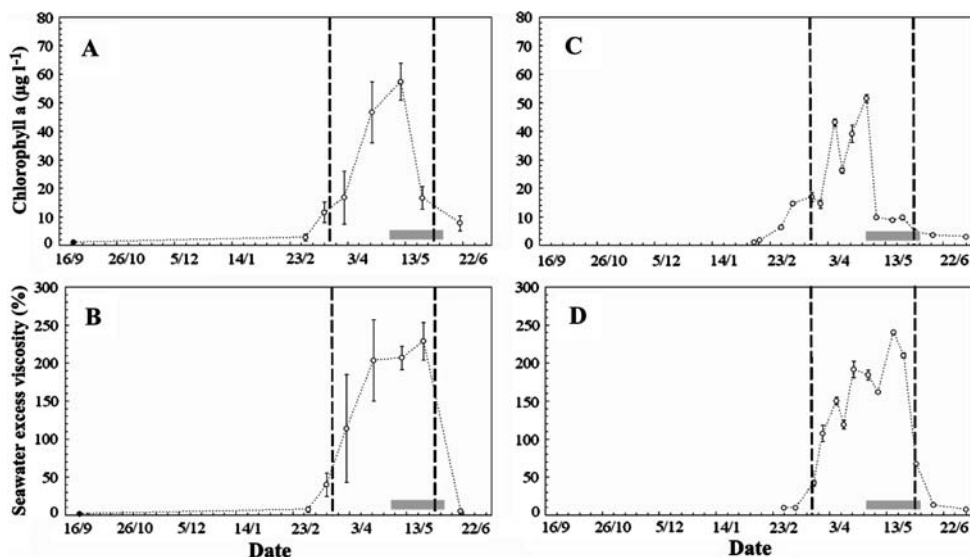
Fig. 5 Time course of chlorophyll *a* concentration (μg l⁻¹; **A**, **C**) and seawater excess viscosity η (%; **B**, **D**), in the intertidal (**A**, **B**; present work) and coastal (**C**, **D**; modified from Seuront et al. 2006) waters of the Eastern English Channel. The grey bar indicates the period of foam formation (May 3 to June 10),

and the dashed vertical lines the appearance and disappearance of *P. globosa* in the phytoplankton assemblage. The sampling conducted on 26 September (black dot; **A**, **B**) has been used as a separate reference sample, characteristic of non-bloom conditions

Table 3 Descriptive statistics of the two-dimensional microscale distributions of chlorophyll *a* concentration (µg l^{-1}) and seawater excess viscosity (%) for each sampling date

Date	Mean	SD	CV	Max./min.
Chlorophyll concentration				
26/09/2003	0.9	0.3	31.4	5.0
05/03/2004	2.7	1.2	44.8	11.9
18/03/2004	11.5	3.6	31.2	11.4
01/04/2004	16.7	9.3	55.8	7.4
20/04/2004	46.6	10.6	22.8	8.1
10/05/2004	57.4	6.5	11.3	2.2
25/05/2004	16.6	4.0	24.0	4.0
20/06/2004	7.7	2.6	33.9	9.7
Excess viscosity				
26/09/2003	1.8	0.7	39.1	16.1
05/03/2004	7.5	3.6	47.6	18.5
18/03/2004	40.1	15.5	38.6	12.1
01/04/2004	113.7	70.9	62.4	15.6
20/04/2004	203.5	53.4	26.3	12.4
10/05/2004	206.8	15.4	7.5	1.7
25/05/2004	228.4	24.9	10.9	2.0
20/06/2004	4.9	3.1	63.6	47.5

SD—standard deviation; CV—coefficient of variation; and max./min.—ratio between the maximum and minimum values of a distribution

Table 4 Results of spatial autocorrelation analyses of chlorophyll *a* and seawater excess viscosity two-dimensional microscale distributions

Date	Moran's I	Geary's c	S^2/ Mean	Distribution	Patch size (cm)
Chlorophyll concentration					
26/09/2003	NS	S+	NS	D	5–10
05/03/2004	NS	NS	S+	E	5–10
18/03/2004	S+	NS	S+	C	5–10
01/04/2004	S+	NS	S+	C	5–10
20/04/2004	S+	S−	S+	A	10–15
10/05/2004	S+	S−	S+	A	10–15
25/05/2004	S+	S−	S+	A	10–15
20/06/2004	NS	S+	S+	D	5–10
Escess viscosity					
26/09/2003	NS	S+	NS	D	5–10
05/03/2004	NS	NS	S+	E	5–10
18/03/2004	S+	NS	S+	C	5–10
01/04/2004	S+	NS	S+	C	5–10
20/04/2004	S+	S−	S+	A	15–20
10/05/2004	S+	S−	S+	A	15–20
25/05/2004	S+	S−	S+	A	15–20
20/06/2004	NS	S+	S+	D	5–10

tration recently investigated, strongly suggests, however, that TEP could play a critical role in the increase in seawater viscosity. The variety of dissolved particulate carbohydrates that are differentially produced during a *Phaeocystis globosa* bloom (see Alderkamp et al. 2005), contribute (for some of them) to the formation of microscopic polymer gels in seawater (Chin et al. 1998) and large sedimenting particles (e.g. TEP; Logan et al. 1995). They may also form an intermediate in the formation of the foam observed after *P. globosa* blooms. The issue of relating quantitative seawater viscosity measurements to the quality and the quantity of dissolved and particulate carbohydrates and transparent exopolymeric particles should then be carefully addressed in the future.

Type of spatial patterns and patch sizes

Spatial autocorrelation and correlograms were used to describe the microscale spatial patterns of chlorophyll *a* concentration and seawater excess viscosity. Identical distribution patterns may or may not produce identical correlograms, while different spatial patterns result in different correlograms (Sokal & Oden 1978b). Both distributions exhibited positive spatial autocorrelation at all the sampling dates. This type of spatial pattern is characterised by an association between extreme and similar per sample values and a transition from high to low values within the sampling area (0.2 m^2). Before and after the spring *P. globosa* bloom the observed spatial patterns (Fig. 2a, d) exclusively exhibited aggregative distributions characterised by the alternation of hot spots and cold spots. The similar increases in patch sizes suggest that the aggregative character of the spatial patterns observed before and after the bloom were mainly due to localised hot spots that may be related to local phytoplankton aggregates (e.g. Koike et al. 1990). In contrast, during the *P. globosa* bloom, and mainly after the formation of foam, these distributions were characterised by a variety of smooth transitions from high to low values. The smoother, more continuous

and structured distributions observed during the bloom and characterised by larger patch sizes may be thought of as: (i) the result of the strong biomodification of the fluid properties mainly by *P. globosa*-related polymeric materials and (ii) a two-dimensional description of the organic matter continuum (Chin et al. 1998; Azam 1998). This is also consistent with the similar patch sizes observed for chlorophyll concentration and excess viscosity before and after the bloom, and the larger excess-viscosity patch sizes observed after the foam formation, when phytoplankton biomass and seawater viscosity appear to be uncoupled.

More generally, microscale hot spots of phytoplankton abundance and/or organic matter concentration may well represent the basis of microhabitats for the development of microbial foodwebs (Thingstad and Billen 1994). Microscale patchiness of organisms attached to aggregates and in the surrounding water column will also fundamentally alter predator-prey and virus-host dynamics, and may subsequently modify the flow of matter through the microbial loop (Azam et al. 1983). The intensity and frequency of these hotspots will also influence the sedimentation processes characterising most *Phaeocystis* sp. blooms (e.g. Andreassen and Wassman 1998) and ultimately determine the proportion of carbon that is sequestered to the sediments or retained in the pelagic food web.

Small-scale versus microscale variability

The temporal patterns observed in the present work for chlorophyll *a* concentration and seawater excess viscosity (Fig. 5a, b) are very similar to those obtained in the coastal waters of the Eastern English Channel, roughly 2 nautical miles offshore, from a standard sampling strategy based on 5 replicate samples taken at three different depth (subsurface, intermediate and bottom waters) using Niskin bottles (Fig. 5c, d; Seuront et al. 2006). This ensures the relevance of the previously proposed mechanisms and generalises them from the scale of the water column down to the microscale. The main difference is the significantly higher chlorophyll concentrations and excess viscosity observed at each sampling date from our intertidal station than from the coastal station (WMW test, $P < 0.05$), which is consistent with the previously observed differences in hydro-

logical properties between intertidal and coastal waters of the Eastern English Channel (Seuront and Spilmont 2002).

The variability observed in chlorophyll *a* concentration and seawater excess viscosity from our microscale (5 cm resolution) two-dimensional sampling is significantly higher than the variability previously estimated at the scale of the water column with a resolution of a few meters (Seuront et al. 2006; see Fig. 5). The coefficient of variation and the ratios between maximum and minimum values are, thus significantly higher at the microscale than at the small-scale (WMW test, $P < 0.01$). More specifically, the ratios between the coefficients of variation (CV) obtained at the microscale and the small-scale range from 2.6 to 42.3 for chlorophyll concentration and from 4.5 to 243.2 for seawater excess viscosity. The ratios between maximum and minimum values are 2.1 to 7.4-fold larger at the microscale than at the small-scale for chlorophyll concentration and 3.1- to 14.3-fold larger at the microscale than at the small scale for excess viscosity. These results are in accordance with previous work showing increased variability and structural complexity with decreasing scale (Seuront and Spilmont 2002; Waters et al. 2003), and indicate that extent of microscale variability amongst marine phytoplankton communities can be greater than the variability observed at larger scales.

These findings are particularly pertinent within the Eastern English Channel as the intense tidal mixing, characterised by turbulent kinetic energy dissipation rates ranging from 10^{-16} to 10^{-4} m^2 s^{-3} (Seuront 2005), is expected to homogenise phytoplankton distributions for scales typically smaller than the depth of the vertically well-mixed water column. Both the extent and the non-random spatial structure of the microscale variability observed here in terms of chlorophyll biomass and seawater excess viscosity imply that phytoplankton organisms, and more specifically *Phaeocystis globosa*, can be independent of the surrounding turbulent flows and induce high levels of spatial heterogeneity, even below the 5 cm scale resolution achieved here.

On the potential role of biologically increased seawater viscosity in *P. globosa* ecology

The impact of turbulence on microorganisms is dependent on its relative size to the smallest

Kolmogorov turbulent eddies defined as $l_k = (v^3/\varepsilon)^{0.25}$, where v is the kinematic viscosity ($m^2\ s^{-1}$) related to the measured viscosity η_m (see Eq. 1) by $v = \eta_m/\rho$ (where η_m and ρ are the fluid viscosity and density, respectively) and ε is the turbulent energy dissipation rate ($m^2\ s^{-3}$). Above this scale the flow is turbulent, while below it, viscosity dominates resulting in a laminar shear. The coastal waters of the Eastern English Channel and the Southern North Sea where *P. globosa* typically flourishes are characterised by elevated turbulent dissipation rates (typically bounded between 10^{-7} and 10^{-4} $m^2\ s^{-3}$; Seuront 2005). These high turbulence intensities and the related sub-millimetre Kolmogorov eddies, ranging from 3.2×10^{-1} to 1.8 mm, are not compatible with the size nor the breakability of *P. globosa* colonies (Peperzak 2002). Mucous secretion, and any subsequent increase in seawater viscosity and Kolmogorov eddy size, may be an environmental engineering strategy that *P. globosa* uses to dampen turbulence, create a favourable, turbulent-free physical habitat to protect colony integrity.

At then end of the bloom, the release of nano-planktonic solitary cells under nutrient limitation would lead to dramatic losses to small protozoan grazers, viruses and zooplankton that would easily offset population growth (Turner et al. 2002). However, excess viscosity remains high, or even increases (Seuront et al. 2006; present work), after colony destruction. This is consistent with the excretion of mucus and dissolved organic carbon observed under nutrient limitation observed in a single cell culture of *P. globosa* (Janse et al. 1999), in colonial cultures of *P. globosa* (van Rijssel et al. 2000) and at the end of *P. pouchetii* blooms in mesocosms (Alderkamp et al. 2005) as well as in many phytoplankton species (Myklestad 1974, 1988). The released flagellated cells may still avoid grazing and viral infection via an alteration of motility and diffusion processes, and a decrease in encounter probabilities and/or in grazing rates attributed, although never demonstrated, to a mechanical hindrance due to increased viscosity (Schoemann et al. 2005). The high-shear environment related to suspensions of aggregates may also be used by *P. globosa* flagellates released from colonies to minimise predation as high shear will decrease their conspicuousness to predators, and not all the perceived preys will be accessible (Seuront et al. 2006).

In addition to colony formation, the exudates released by *P. globosa* and the subsequent increase in viscosity might then also be considered as a potential antipredator adaptive strategy that ultimately ensures the completion of its life cycle in highly turbulent environments.

In the sea, the viscous properties of most polymers and suspensions of aggregates are generally dependent on deformation rate. The biologically induced excess viscosity η_{Bio} (see Eq. 3) is then related to the shear γ (s^{-1}) as (Jenkinson 1986) $\eta_{Bio} = k\gamma^{-P}$, where k is a constant, $\gamma = (\varepsilon/v)^{0.5}$ with $v = 10^{-6}$ $m\ s^{-1}$, and P has so far been found to lie between 0 and 1.6 (e.g. Jenkinson and Biddanda 1995), or even as low as -0.2 (Jenkinson et al. 1998). A single value of P ($P = 1.11$) has been derived from 15 samples taken in the German Bight when *Phaeocystis* sp. was blooming (Jenkinson 1993). Considering the lack of information related to the value of P for *Phaeocystis globosa*, the intrinsic plurispecific and dynamic nature of the phytoplankton assemblages, the range of P values proposed in the literature and the range of turbulence intensities found in *P. globosa* natural environment (i.e. $\varepsilon = 10^{-7}$ to 10^{-4} $m^2\ s^{-3}$, Seuront 2005), any attempt to quantify the nontrivial effect of excess viscosity on the Kolmogorov scale and related microscale processes is still unreasonable at this time. Future investigations should, however, focus on the potential differential contribution of the different carbohydrates that are differentially produced during a *Phaeocystis globosa* bloom (see Alderkamp et al., 2007) to the observed increase in seawater viscosity.

Conclusions

The present work suggests that *Phaeocystis globosa* has developed specific adaptive strategies to favourably modify its immediate microenvironment. The consequences of this strategy are far-reaching as they have been shown to modify the microscale variability of chlorophyll concentration and seawater excess viscosity for scales ranging from 5 to 45 cm. In particular, the modification of the extent and the non-random spatial structure of the microscale variability observed here in terms of chlorophyll biomass and seawater excess viscosity over the course of a *Phaeocystis globosa* spring bloom imply that phytoplankton in general, and more specifically *P. globosa*,

can induce high levels of spatial heterogeneity. The microscale adaptive processes discussed here are thus likely to cascade from the cell and/or colony scales up to larger scale and to influence critical processes such as biogeochemical fluxes through their impact on, e.g. sedimentation and remineralisation processes, and predator-prey and virus-host dynamics. It is finally stressed that our journey to elucidate the relationship between seawater viscous properties and the plankton components is only beginning, and that the future of plankton rheology should rely on interdisciplinary efforts focusing on seawater rheological properties (including viscosity and elasticity) as well as on phytoplankton taxonomy and standing stock, *P. globosa* colony size, turbulence intensity and the quality and quantity of exopolymeric materials.

References

Al-Hasan RH, Ali AM, Radwan SS (1990) Lipids, and their constituent fatty acids, of *Phaeocystis* sp. From the Arabian Gulf. Mar Biol 105:9–14

Alderkamp AC, Buma AGJ, van Rijssel M (2007) The carbohydrates of Phaeocystis and their degradation in the microbial food web. Biogeochemistry, doi:10.1007/s10533-007-9078-2

Alderkamp AC, Nejstgaard JC, Verity PG, Zirbel MJ, Sazhin AF, van Rijssel M (2005) Dynamics in carbohydrate composition of Phaeocystis pouchetii colonies during spring blooms in mesocosm. J Sea Res 55:169–181

Andreassen IJ, Wassman P (1998) Vertical flux of phytoplankton and particulate biogenic matter in the marginal zone of the Barents Sea in May 1993. Mar Ecol Prog Ser 170:1–14

Azam F (1998) Microbial control of oceanic carbon flux: the plot thickens. Science 280:694–696

Azam F, Fenchel T, Field JG, Gray JS, Meyer-Reil LA, Thingstad F (1983) The ecological role of water-column microbes in the sea. Mar Ecol Prog Ser 10:257–263

Brylinski JM, Lagadeuc Y, Gentilhomme V, Dupont JP, Lafite R, Dupeuple PA, Huault MF, Auger Y, Puskaric E, Wartel M, Cabioch L (1991) Le 'fleuve côtier': un phénomène hydrologique important en Manche orientale (exemple du Pas de Calais). Oceanol Acta 11:197–203

Buskey EJ 1998. Components of mating behavior in planktonic copepods. J Mar Syst 15:13–21

Cartamil DP, Lowe CG (2004) Diel movement patterns of ocean sunfish *Mola mola* off southern California. Mar Ecol Prog Ser 266:245–253

Chin WC, Orellana MV, Verdugo P (1998) Spontaneous assembly of marine dissolved organic matter into polymer gels. Nature 391:568–572

Decho A, Fleeger J (1988) Microscale dispersion of meiobenthic copepods in response to food-resource patchiness. J Exp Mar Biol Ecol 118:229–243

Dekshenieks MM, Donaghay PL, Sullivan JM, Rines JEB, Osborn TR, Twardowski MS (2001) Temporal and spatial occurrence of thin phytoplankton layers in relation to physical processes. Mar Ecol Prog Ser 223:61–71

Dreyfuss R (1962) Note biologique à propos des eaux rouges. Cah Cent Rech Biol Océanogr Méd Nice 1:14–15

Geary RC (1954) The contiguity ratio and statistical mapping. Incop Statist 5:115–145

Janse I, van Rijssel M, Ottema A, Gottschal JC (1999) Microbial breakdown of *Phaeocystis* mucopolysaccharides. Limnol Oceanogr 44:1447–1457

Jenkinson IR (1986) Oceanographic implications of non-Newtonian properties found in phytoplankton cultures. Nature 323:435–437

Jenkinson IR (1993) Bulk-phase viscoelastic properties of seawater. Oceanol Acta, 16:317–334

Jenkinson IR, Biddanda BA (1995) Bulk-phase viscoelastic properties of seawater: relationship with plankton components. J Plankton Res 17:2251–2274

Jenkinson IR, Wyatt T, Malej T (1998) How viscoelastic effects of colloidal biopolymers modify rheological properties of seawater. In: Emri I, Cvelbar R (eds) Proceedings of the 5th European Rheology Conference, Portoroz, Slovenia, September 6–11, 1998, Progress and Trends in Rheology 5:57–58

Koike I, Shigemitsu H, Kazuki T, Kogure K (1990) Role of sub-micrometer particles in the ocean. Nature 345:242–244

Lancelot C, Billen G, Sournia A, Weisse T, Colijn F, Veldhuis MJW, Davies A, Wassman P (1987) *Phaeocystis* blooms and nutrient enrichment in the continental zones of the North Sea. Ambio 16:38–46

Legendre P, Legendre L (1998) Numerical ecology. Elsevier, New York

Levin SA (1992) The problem of patterns and scale in ecology. Ecology 73:1943–1967

Logan BE, Passow U, Alldredge AL, Grossard HP, Simon M (1995) Rapid formation and sedimentation of large aggregates is predictable from coagulation rates (half-lives) of transparent exopolymer particles (TEP). Deep-Sea Res 42:203–214

Mari X, Rassoulzadegan F, Brussaard CPD, Wassmann P (2005) Dynamics of transparent exopolymeric particles (TEP) production by *Phaeocystis globosa* under N- or P-limitation: a controlling factor of the retention/export balance. Harmful Algae 4:895–914

Martin AP (2003) Phytoplankton patchiness: the role of lateral stirring and mixing. Prog Oceanogr 57:125–174

Miyake Y, Koizumi M (1948). The measurements of the viscosity coefficient of sea water. J Mar Res 7:63–66

Myklestad S (1974) Production of carbohydrates by marine planktonic diatoms. I. Comparison of nine different species in culture. J Exp Mar Biol Ecol 15:261–274

Myklestad SM (1988) Production, chemical structure, metabolism, and biological function of the (1,3)-linked, beta-D-glucans in diatoms. BiolOceanogr 6:313–326

Moran PAP (1950) Notes on continuous stochastic phenomena. Biometrika 37:17–23

Peperzak L (2002) The wax and wane of *Phaeocystis globosa* blooms. Ph.D. Thesis, University of Groningen, The Netherland

Schoemann V, Becquevort S, Stefels J, Rousseau V, Lancelot C (2005) *Phaeocystis* blooms in the global ocean and their controlling mechanisms: a review. J Sea Res 53:43–66

Seuront L (2005) Hydrodynamic and tidal controls of small-scale phytoplankton patchiness. Mar Ecol Prog Ser 302:93–101

Seuront L, Spilmont N (2002) Self-organized criticality in intertidal microphytobenthos patch patterns. Physica A 313:513–539

Seuront L, Schmitt F, Lagadeuc Y (2001) Turbulence intermittency, small-scale phytoplankton patchiness and encounter rates in plankton: where do we go from here? Deep-Sea Res I 43:1199–1215

Seuront L, Vincent D, Mitchell JG (2006) Biologically-induced modification of seawater viscosity in the Eastern English Channel during a *Phaeocystis globosa* spring bloom. J Mar Syst 61:118–133

Seymour JR, Mitchell JG, Pearson L, Waters RL (2000) Heterogeneity in bacterioplankton abundance from 4.5 millimetre resolution sampling. Aquat Microb Ecol 22:143–153

Sokal R, Oden N (1978a) Spatial autocorrelation in biology. I Methodology Biol J Linn Soc London 10:199–228

Sokal R, Oden N (1978b) Spatial autocorrelation in biology. II. Some biological implications and four applications of evolutionary and ecological interest. Biol J Linn Soc London 10:229–249

Sokal RR, Rohlf FJ (1995) Biometry. The principles and practice of statistics in biological research. Freeman, San Francisco

Strickland JDH, Parsons TR (1972) A practical handbook of seawater analysis. Bull Fish Res Bd Canada 167:1–311

Suzuki R, Ishimaru T (1990) An improved method for the determination of phytoplankton chlorophyll using N, N-Dimethylformamide. J Oceanogr Soc Japan 46:190–194

Tiselius P (1992) Behavior of *Acartia tonsa* in patchy food environments. Limnol Oceanogr 8:1640–1651

Thingstad TF, Billen G (1994) Microbial degradation of *Phaeocystis* material in the water column. J Mar Syst 5:55–65

Turner JT, Ianora A, Esposito F, Carotenuto Y, Miralto A (2002) Zooplankton feeding ecology: does a diet of *Phaeocystis* support good copepod grazing, survival, egg production and egg hatching success? J. Plankton Res 24:1185–1195

van Rijssel M, Janse I, Noordkamp DJB, Gieskes WWC (2000) An inventory of factors that affect polysaccharide production by *Phaeocystis globosa*. J Sea Res 43:297–306

Verity PG, Medlin LK (2003) Observations on colony formation by the cosmopolitan phytoplankton genus *Phaeocystis*. J Mar Syst 43:153–164

Waters RL, Mitchell JG, Seymour JR (2003) Geostatistical characterisation of centimetre-scale spatial stucture of in vivo fluorescence. Mar Ecol Prog Ser 251:49–58

Zar JH (1996) Biostatistical analysis. Prentice Hall, NJ